

ANALYSIS OF THE HALL AND ION-SLIP EFFECTS IN A MHD CHANNEL FLOW: A HYBRID APPROACH

Bruno N.M. da Silva ^{*}, Gustavo E. Assad ^{**} and João A. de Lima ^{***,§}

^{*}Post-Graduate Program of Mech. Eng., UFRN, Natal-RN, Brazil

^{**}Federal Institute of Technology, IF/PB, João Pessoa-PB, Brazil

^{***}Renewable Energy Engineering Department, UFPB/CEAR, João Pessoa-PB Brazil

[§]Correspondence author. Phone: +55 83 3216-7127 Email: jalima@cear.ufpb.br

ABSTRACT This paper reports the development of a hybrid (generalized integral transform) solution to the unsteady magneto-convection problem of an electrically conducting Newtonian fluid, with temperature-dependent transport properties, within a channel in which Hall and ion-slip effects are taken into account. Hall effects are important when the ratio between the fluid electron-cyclotron frequency and the electron-atom-collision frequency is high (the Hall parameter). Also, when the electromagnetic force is very large, the diffusion velocity of ions may also not be negligible. If the diffusional velocity of ions and electrons are included, we have the phenomena of ion slip. In spite of these phenomena, it is considered that the magnetic Reynolds number is small, i.e., the flow-induced magnetic fields are not enough strong to modify the applied transversal magnetic field. Here, in order to cover a broader range of problems, a time dependent pressure gradient, an inflow perpendicular to the plates (porous) and a non-zero upper plate velocity are also considered in the mathematical formulation. Results are illustrated and compared to the main numerical results from the literature for the related velocity and temperature potentials as function of the main governing parameters, namely, Hartmann, suction/injection, transport properties and electron and ion-slip parameters. In order to illustrate the consistency of the technique (GITT) and its use for benchmarking purposes in the area of magneto fluid dynamics, convergence analyses are carried out for the main potentials.

INTRODUCTION

Appearing in the early twentieth century, interest in magnetohydrodynamics of electric conductive fluids (MHD) reappeared in the 1960s, and is currently the subject of several computational and experimental scientific investigations, mainly due to energy and environmental issues. Magnetohydrodynamics is present in a number of areas, from geophysics to nuclear engineering to metallurgical and materials engineering. Magnetohydrodynamics is present in a number of engineering applications to control, suppress, drive, and generate motion involving electrically conducting fluids [Shercliff, 1965; Davidson, 2001; Sutton and Sherman, 2006].

Channel flows are present in several technological devices and it is the geometric configuration that is usually employed by computational approaches for benchmarking purposes. In a general way, simplified MHD-flow configurations were analyzed and then others physical features were added to the previous formulations, so that more insight on the physical aspects of the flow and magnetic fields was obtained and numerical difficulties were imposed. For example, the MHD steady-state fully-developed porous-plate Couette flow with pressure gradient and heat transfer of a

temperature-exponentially-varying viscosity fluid was studied by Attia and Kotb [1996]. Later on, Attia [2006a] neglected plate porosities and analyzed the problem by considering that viscosity, thermal and electrical conductivities were temperature-dependent. Hall and ion-slip effects were considered in the study of the Hartmann plane-Poiseuille fully-developed flow with heat transfer by Attia [2003]. As in the first work, the viscosity was an exponential function of temperature.

Analysis of the unsteady-state regime was firstly introduced by Attia [1999] who studied the transient MHD plane-Poiseuille flow with heat transfer under a temperature-varying viscosity. Later, the problem was extended to incorporate the Hall effect [Attia, 2005a] and the Hall effect and temperature-dependency for all transport properties [Attia and Aboul-Hassan, 2003]. Hall and ion-slip effects were simultaneously considered by Attia [2006b] in a work that considered constant the transport properties and brought back the hypothesis of porous plates. Also, the unsteady Hartmann plane-Poiseuille flow with heat transfer considered was driven by an exponentially-decaying pressure gradient. Unsteady Couette flow with heat transfer and variable properties and Hall effects was studied by Attia [2008a]. Following the same trend of analysis, Attia [2002], Attia [2005b], Attia [2005c], Attia [2006c], Attia [2008b], and Attia *et al.* [2015], among others, extended the previous studies for dusty flows with particles in suspension such as ash or soot.

All the previous studies employed some sort of numerical method, or approximate approach such as the regular perturbation method, to solve the governing equations. Although it is not the case for the problems above referenced, solution procedures to the magnetohydrodynamic multi-physic equations (the Navier-Stokes and the Maxwell equations, in a more general formulation, even with the MHD simplifications) normally face some numerical or limiting problems related to the strong coupling between the flow and the magnetic equations, and the nonlinear nature of these equations. On the other hand, hybrid methods such as the so-called Generalized Integral Transform Technique (GITT) have been employed to solve heat and fluid flow problems with relative success. GITT is a numerical-analytical method that keeps all the characteristics of an analytical solution (similar to the method of separation of variables), associated with the robustness of the purely numerical methods for solution of systems of ordinary differential equations (when solving systems of partial differential equations). Combined with its automatic global error control, the technique is a reliable alternative for obtaining benchmark results, as it has been demonstrated along the years [Ozisik & Murray, 1974; Mikhailov & Ozisik, 1984; Cotta, 1993; Cotta, 1998; Santos *et al.*, 2001].

Application of the integral transform method in the field of magnetohydrodynamics can be assessed after the work of Lima *et al.* [2007], who worked in the same problems studied by Attia and Kotb [1996] and Attia [1999], and the work of Lima & Rêgo [2013], who studied the steady-state simultaneously developing force convection in the entrance region of a parallel-plate channel using a boundary layer formulation and compared their results with the numerical results of Shohet *et al.* [1962], Hwang *et al.* [1966], and Setayesh & Sahai [1990] for different physical situations.

The main goal of the present work is, therefore, to extend the range of physical problems that can be handled with the integral transform method, showing its outstanding characteristics for benchmark purposing. Specifically, this is attained by illustrating convergence analyses and comparing results for the unsteady Hartmann plane-Poiseuille or Couette flow with Hall and ion-slip effects with other numerical findings for the main potentials, as function of the governing parameters, namely, Hartmann, suction/injection, and electron and ion-slip parameters. It must be made clear that despite accounting for Hall and ion-slip effects, it is still considered that the electric currents induced in the flow field are not strong enough to alter the applied external magnetic field, i.e., the hypothesis of small magnetic Reynolds number is adopted. To cover a broader range of physical situations, it is used a formulation in which fluid suction/ejection through the channel walls, exponentially-varying pressure gradient as well as temperature-dependent transport properties can occur.

MATHEMATICAL FORMULATION

By considering a rectangular channel in which the two horizontal plates are insulated, porous or not, separated by a distance h , kept at constant temperatures (different or not), and the two vertical plates are electrical conductors to which a resistive load/electrical source can be connected, the governing equations (and the corresponding initial and boundary conditions) are written in dimensionless form as:

$$\frac{\partial u}{\partial t} + R_v \frac{\partial u}{\partial y} = -\frac{\partial P}{\partial x} + \frac{\partial}{\partial y} \left(\mu[T] \frac{\partial u}{\partial y} \right) - \frac{Ha^2 \sigma[T]}{(1+\beta_e \beta_i)^2 + \beta_e^2} [(1+\beta_e \beta_i)(E_z + u) + \beta_e w] \quad (1)$$

$$\frac{\partial w}{\partial t} + R_v \frac{\partial w}{\partial y} = \frac{\partial}{\partial y} \left(\mu[T] \frac{\partial w}{\partial y} \right) - \frac{Ha^2 \sigma[T]}{(1+\beta_e \beta_i)^2 + \beta_e^2} [(1+\beta_e \beta_i)w - \beta_e(E_z + u)] \quad (2)$$

$$\frac{\partial T}{\partial t} + R_v \frac{\partial T}{\partial y} = \frac{1}{Pr} \frac{\partial}{\partial y} \left(k[T] \frac{\partial T}{\partial y} \right) + Ec \mu[T] \left\{ \left(\frac{\partial u}{\partial y} \right)^2 + \left(\frac{\partial w}{\partial y} \right)^2 \right\} + \frac{Ec Ha^2 \sigma[T]}{(1+\beta_e \beta_i)^2 + \beta_e^2} [(E_z + u)^2 + w^2] \quad (3)$$

$$u(y, 0) = 0, \quad w(y, 0) = 0, \quad T(y, 0) = 0 \} ; \quad t = 0, \quad 0 < y < 1 \quad (4.a-c)$$

$$u(0, t) = 0, \quad w(0, t) = 0, \quad T(0, t) = 0 \} ; \quad y = 0, \quad t > 0 \quad (5.a-c)$$

$$u(1, t) = R_u, \quad w(1, t) = 0, \quad T(1, t) = 1 \} ; \quad y = 1, \quad t > 0 \quad (6.a-c)$$

The following dimensionless groups were adopted in the above equations:

$$\begin{aligned} x^* &= \frac{x^*}{h}, & y^* &= \frac{y^*}{h}, & u &= \frac{u^* h}{V_1^*}, & w &= \frac{w^* h}{V_1^*}, & t &= \frac{t^* V_1^*}{h^2}, & R_u &= \frac{u_2^* h}{V_1^*}, & R_v &= \frac{v_0^* h}{V_1^*}, & P &= \frac{h^2 P^*}{\rho V_1^{*2}}, \\ T &= \frac{T^* - T_1^*}{T_2^* - T_1^*}, & \mu &= \frac{\mu^*}{\mu_1^*}, & k &= \frac{k^*}{k_1^*}, & \sigma &= \frac{\sigma^*}{\sigma_1^*}, & Pr &= \frac{k_1^*}{\mu_1^* c_p}, & Ec &= \frac{V_1^{*2}}{h^2 c_p (T_2^* - T_1^*)}, & E_z &= \frac{h}{V_1^*} \frac{E_0}{B_0} \end{aligned} \quad (7)$$

In these groups, Ha , Pr and Ec stand to Hartmann, Prandtl and Eckert numbers, and β_e and β_i , in the last terms of the governing equations, are the Hall and ion-slip parameters, respectively. R_u and R_v are the dimensionless upper-wall and wall suction/ejection velocities, respectively. Flow can be sustained by a constant or a time-decaying pressure gradient, and since the magnetic Reynolds number is considered small, there is no induced magnetic field. Indices 1 and 2 refer to properties evaluated at the bottom- and upper-wall temperatures, respectively.

The pressure gradient that drives the flow and the transport properties are given as follows:

$$\frac{\partial P}{\partial x}(t) = G_0 \left(e^{-i_{\alpha G} \alpha_G t} \right) \quad (8.a)$$

$$\mu(T) = e^{-a T}, \quad k(T) = 1 + b T, \quad \sigma(T) = 1 + c T \quad (8.b-d)$$

G_0 is the constant pressure gradient and $i_{\alpha G}$ is a flag parameter that indicates if the pressure gradient is a function of time ($i_{\alpha G} = 1$) or not ($i_{\alpha G} = 0$), α_G being the time-decaying factor.

INTEGRAL TRANFORM SOLUTION PROCEDURE

Splitting up of Potentials To take full advantage of its hybrid nature, the integral transform method requires that the boundary conditions in the direction to be integral transformed be homogeneous. This is a requirement associated to the corresponding eigenvalue problem. Since the

boundary conditions at the upper-plate are inhomogeneous, the following splitting up of the longitudinal velocity component and temperature is proposed:

$$u(y,t) = u_h(y,t) + u_F(y) \quad (9.a)$$

$$T(y,t) = T_h(y,t) + T_F(y) \quad (9.b)$$

$u_h(y,t)$ and $T_h(y,t)$ are the homogenized (the filtered) potentials, and $u_F(y)$ and $T_F(y)$ are solutions (the filtering functions) of simplified steady-state versions of the original equations, which must bring the inhomogeneity. Here, they were chosen as:

$$0 = -G_0(1 - i_{\alpha G}) + \frac{\partial^2 u_F}{\partial y^2} - Ha^2(E_z + u_F), \quad \begin{cases} u_F(0) = 0 \\ u_F(1) = R_u \end{cases} \quad (10.a-c)$$

$$0 = \frac{d^2 T_F}{dy^2}, \quad \begin{cases} T_F(0) = 0 \\ T_F(1) = 1 \end{cases} \quad (11.a-c)$$

Their solutions are easily obtained as (making $G_G = G_0(1 - i_{\alpha G}) + Ha^2 E_z$):

$$u_F(y) = \begin{cases} \frac{G_G(1 - \cosh[Ha y]) + \left\{ G_G(\cosh[Ha] - 1) + Ha^2 R_u \right\} \frac{\sinh[Ha y]}{\sinh[Ha]}}{Ha^2}, & Ha \neq 0 \\ \frac{G_G}{2}(y - y^2) + R_u y, & Ha = 0 \end{cases} \quad (12)$$

$$T_F(y) = y \quad (13)$$

This procedure automatically guarantees the GITT requirements of homogeneity of boundary conditions and, additionally, reduces the convergence needing as the fully-developed steady-state regime is approaching.

Integral Transformation After the splitting up procedure, the equations must be integral transformed through use of the eigenfunctions and the orthogonality properties associated to the appropriate eigenvalue problems. The following eigenvalue problem was adopted to all potentials:

$$\frac{d^2 \tilde{\psi}_i(y)}{dy^2} = \lambda_i^2 \tilde{\psi}_i(y), \quad \begin{cases} \tilde{\psi}_i(0) = 0 \\ \tilde{\psi}_i(1) = 0 \end{cases} \quad (14.a-c)$$

This eigenvalue problem has the following properties:

$$\psi_i(y) = \frac{\tilde{\psi}_i(y)}{N_i^{1/2}} = \sqrt{2} \sin(\lambda_i y), \quad \begin{cases} \lambda_i = i\pi, & i = 1, 2, 3, \dots \\ \int_0^1 \tilde{\psi}_i(y) \tilde{\psi}_j(y) dy = \begin{cases} 0, & i \neq j \\ N_i = 1/2, & i = j \end{cases} \end{cases} \quad (15.a-c)$$

Then, it is proposed the following integral transform/inverse pairs for velocity and temperature:

$$\begin{cases} u_h(y,t) = \sum_{i=1}^{\infty} \psi_i(y) \bar{u}_{hi}(t) \\ \bar{u}_{hi}(t) = \int_0^1 \psi_i(y) u_h(y,t) dy \end{cases}, \quad \begin{cases} w(y,t) = \sum_{i=1}^{\infty} \psi_i(y) \bar{w}_i(t) \\ \bar{w}_i(t) = \int_0^1 \psi_i(y) w(y,t) dy \end{cases}, \quad \begin{cases} T_h(y,t) = \sum_{i=1}^{\infty} \psi_i(y) \bar{T}_{hi}(t) \\ \bar{T}_{hi}(t) = \int_0^1 \psi_i(y) T_h(y,t) dy \end{cases} \quad (16.a-f)$$

To be integral transformed, the homogenized versions of the governing equations are firstly multiplied by the eigenfunctions and then integrated over the domain ($\int_0^1 \psi_i(y) (Eqs.) dy$), resulting in the following transformed system of coupled EDOs and respective transformed initial conditions:

$$\frac{d\bar{u}_{hi}(t)}{dt} = G_0 \bar{f}_i \left(e^{-i_{\alpha G} \alpha_G t} \right) + \bar{B}_{ui}, \quad \bar{u}_{hi}(0) = -\bar{h}_i, \quad i=1, 2, 3, \dots, \infty \quad (17.a, b)$$

$$\frac{d\bar{w}_i(t)}{dt} = \bar{B}_{wi}, \quad \bar{w}_i(0) = 0, \quad i=1, 2, 3, \dots, \infty \quad (17.c, d)$$

$$\frac{d\bar{T}_{hi}(t)}{dt} = \bar{B}_{Ti}, \quad \bar{T}_{hi}(0) = -\bar{g}_i, \quad i=1, 2, 3, \dots, \infty \quad (17.e, f)$$

The transformed coefficients are written as follows:

$$\bar{f}_i = \int_0^1 \psi_i(y) dy = -\frac{\sqrt{2}}{\lambda_i} \left[(-1)^i - 1 \right] \quad (18.a)$$

$$\bar{h}_i = \int_0^1 \psi_i(y) u_F(y) dy = \frac{\sqrt{2} \left(G_G - (-1)^i \left[G_G + \lambda_i^2 R u \right] \right)}{\lambda_i \left(H a^2 + \lambda_i^2 \right)} \quad (18.b)$$

$$\bar{g}_i = \int_0^1 \psi_i(y) T_F(y) dy = -\frac{\sqrt{2}}{\lambda_i} (-1)^i \quad (18.c)$$

$$\bar{B}_{ui} = - \int_0^1 \left\{ \left(\psi_i R v + \dot{\psi}_i \mu[T] \right) \frac{\partial u}{\partial y} + \psi_i \frac{H a^2 \sigma[T]}{(1 + \beta_i \beta_e)^2 + \beta_e^2} \left[(1 + \beta_i \beta_e)(E_z + u) + \beta_e w \right] \right\} dy \quad (18.d)$$

$$\bar{B}_{wi} = - \int_0^1 \left\{ \left(\psi_i R v + \dot{\psi}_i \mu[T] \right) \frac{\partial w}{\partial y} + \psi_i \frac{H a^2 \sigma[T]}{(1 + \beta_i \beta_e)^2 + \beta_e^2} \left[(1 + \beta_i \beta_e)w - \beta_e (E_z + u) \right] \right\} dy \quad (18.e)$$

$$\bar{B}_{Ti} = - \int_0^1 \left\{ \left(\psi_i R v + \dot{\psi}_i k[T] \right) \frac{\partial T}{\partial y} + \psi_i E c \left\{ \mu[T] \left[\left(\frac{\partial u}{\partial y} \right)^2 + \left(\frac{\partial w}{\partial y} \right)^2 \right] + \frac{H a^2 \sigma[T]}{(1 + \beta_i \beta_e)^2 + \beta_e^2} \left[(E_z + u)^2 + w^2 \right] \right\} \right\} dy \quad (18.f)$$

If each eigen-expansion is truncate in a finite number of terms, $NU=NW=NT=N$, then we have a final coupled system of $3N$ first order ordinary differential equations.

RESULTS AND DISCUSSION

To solve the transformed system represented by Eqs. (17) and (18), a Fortran 90 code was developed and routine IVPAG [IMSL, 2010] was employed prescribing an error target of 10^{-8} as the tolerance criterion. This routine is appropriate to handle stiff initial-value problems. The non-transformable integral coefficients, Eqs. (18.d-f), are dynamically obtained through routine FQRUL [IMSL, 2010] that uses Fejer-quadrature rules for numerical integration. NQR=10,000 points of quadrature were used in order to guarantee that all coefficients be evaluated within the appropriate accuracy.

Results for the longitudinal and transversal velocity components, temperature, and longitudinal and transversal skin friction coefficients, and Nusselt number, at the bottom and upper plates are evaluated according to their definition, the relation with the inverse formulae and the filtering expressions, for different combinations of the governing parameters ($Ha, G_o, \alpha_G, i_{\alpha G}, R_u, R_v, Pr, Ec, E_z, a, b, c, \beta_e, \beta_i$) as:

$$u(y,t) = \sum_{i=1}^{\infty} \psi_i(y) \bar{u}_{hi}(t) + u_F(y) ; \quad w(y,t) = \sum_{i=1}^{\infty} \psi_i(y) \bar{w}_i(t) \quad (16.a,c)$$

$$T(y,t) = \sum_{i=1}^{\infty} \psi_i(y) \bar{T}_{hi}(t) + T_F(y) \quad (16.e)$$

$$\tau_{x0} = \left. \frac{\partial u}{\partial y} \right|_{y=0} = \sum_{i=1}^{\infty} \psi_i(0) \bar{u}_{hi}(t) + u_F(0) ; \quad \tau_{x1} = \left. \frac{\partial u}{\partial y} \right|_{y=1} = \sum_{i=1}^{\infty} \psi_i(1) \bar{u}_{hi}(t) + u_F(1) \quad (19.a,b)$$

$$\tau_{y0} = \left. \frac{\partial w}{\partial y} \right|_{y=0} = \sum_{i=1}^{\infty} \psi_i(0) \bar{w}_i(t) ; \quad \tau_{y1} = \left. \frac{\partial w}{\partial y} \right|_{y=1} = \sum_{i=1}^{\infty} \psi_i(1) \bar{w}_i(t) \quad (20.a,b)$$

$$Nu_0 = \left. \frac{\partial T}{\partial y} \right|_{y=0} = \sum_{i=1}^{\infty} \psi_i(0) \bar{T}_{hi}(t) + T_F(0) ; \quad Nu_1 = \left. \frac{\partial T}{\partial y} \right|_{y=1} = \sum_{i=1}^{\infty} \psi_i(1) \bar{T}_{hi}(t) + T_F(1) \quad (21.a,b)$$

Figures 1.a and 1.b depict comparisons for the velocity profile with the findings of Attia [2006a], for the generalized steady-state Couette flow. Results are compared for $Ha = 2$ and 6 , $G_o = 40$, $\alpha_G = 0$ ($i_{\alpha G} = 0$), $R_u = 2$, $R_v = 0$, $Pr = 1$, $Ec = 0.05$, $E_z = 0$, $b = 0$, $\beta_e = 0$, $\beta_i = 0$ and different values of viscosity parameter, a , and electrical conductivity parameter, c . Additional comparisons for this geometry can be found in the work of Lima *et al.* [2007] who reproduced the results of Attia and Kotb [1996]. Figure 1.a illustrates the case for $a = -0.5$ and Fig. 1.b for $a = 0.5$.

In these and in subsequent graphs, subscript A stands to result/variable relative to the reference used for comparisons, most of them due to Attia, who used different characteristic scales for definition of his dimensionless parameters.

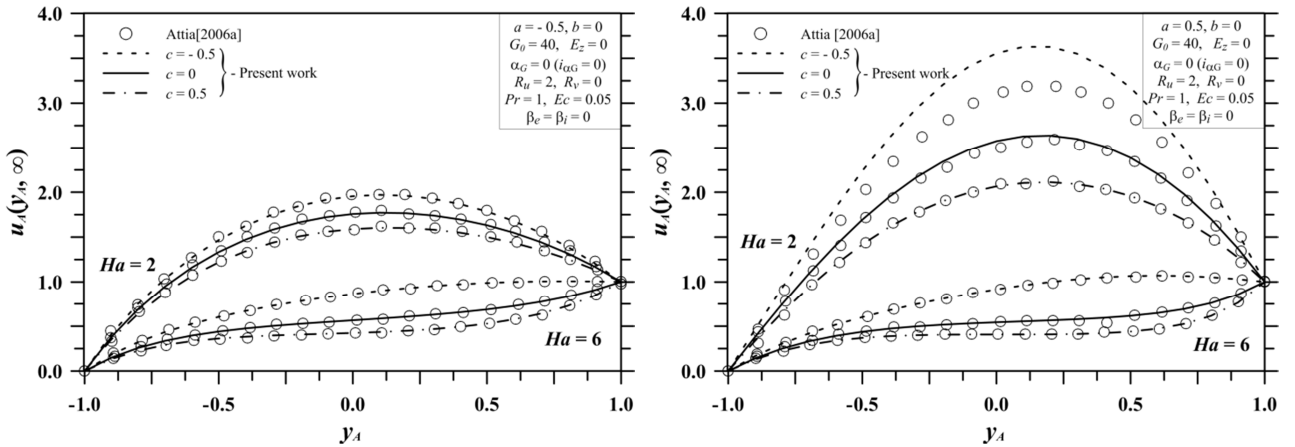


Figure 1. Axial velocity component profiles for the steady-state Couette flow for different values of Hartmann, Ha , and properties parameters a and c .

These figures show the strong influence of the magnetic field (Hartmann number) and the transport properties parameters (a and c) on the velocity profile. As one would expect, an increase in Ha promotes a strong reduction on the velocity field (the retarding Lorentz force effect). This effect is more intensified by decreasing the viscosity parameter (which makes the viscosity to increase with temperature) and increasing the electrical conductivity parameter (which makes the electrical conductivity to increase with temperature, and thus increasing the retarding Lorentz force).

It is noticed in Fig. 1.b slight differences between the results for the case of higher viscosity parameter, $a = 0.5$, lower electrical parameter, $c = -0.5$ and smaller Hartmann number, $Ha = 2$. As the problem here studied is quite simple, it is believed that the results presented by Attia [2006a] contain some error attributed to his numerical method (maybe they are not fully converged) or were obtained from a simulation with different values of the viscosity and/or electrical parameters.

To show that this is the case, Table 1 shows a comparison for the temperature at the channel centerline for the simplest situation, *i.e.*, constant physical properties ($a = b = c = 0$) and no Hall and ion-slip effects ($\beta_e = \beta_i = 0$) for $Ha = 2$ and $Ha = 6$, for which analytical solution can be easily obtained using software Mathematica [Wolfram, 2010], for example. According to this table, results of Attia (2006a) are not fully converged, even for the steady-state regime, so one can believe that inaccuracies may be present in more complex situations.

Table 1
Steady-state temperature at the channel centerline for the simplest cases

Ha	$T(0, \infty)$		
	Analytical solution	Present work	Attia [2006a]
2	1.03204	1.03204	1.0333
6	0.791964	0.791964	0.7925

Results for the unsteady flow regime with heat transfer considering variable properties and Hall effects are now illustrated and compared to the findings of Attia [2008a], for Couette flow, and of Attia & Aboul-Hassan [2003] and Attia [2005a], for plane-Poiseuille flow.

Figures 2 and 3 compare the results for the longitudinal and transversal velocity component profiles, respectively, for $Ha = 2$, $G_0 = 40$, $\alpha_G = 0$ ($i_{\alpha G} = 0$), $R_v = 0$, $Pr = 1$, $Ec = 0.05$, $E_z = 0$, $a = 0.5$, $b = 0.5$, $c = 0$, $\beta_e = 3$, $\beta_i = 0$ at different instant of time, for generalized Couette ($R_u = 2$) and plane-Poiseuille ($R_u = 0$) flows. One can observe the excellent matching between the present hybrid results and the numerical ones. Physically, except for the kind of boundary conditions used, there are no substantial differences between the two flow configurations and also, although not shown, alterations on the temperature field from the Couette to the plane-Poiseuille flow configuration are very subtle.

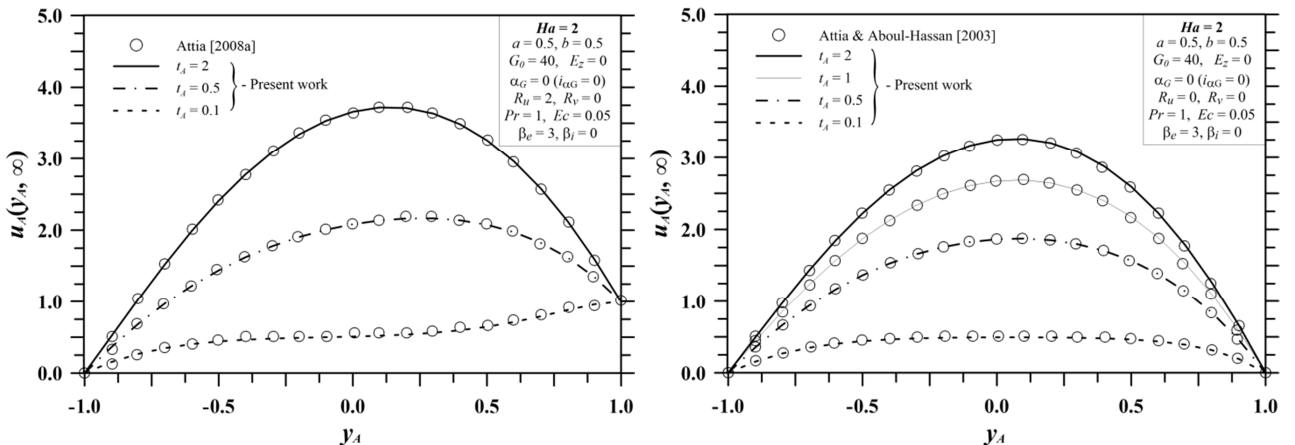


Figure 2. Longitudinal velocity profiles for the unsteady (a) Couette and (b) plane-Poiseuille flow at different times for $Ha = 2$.

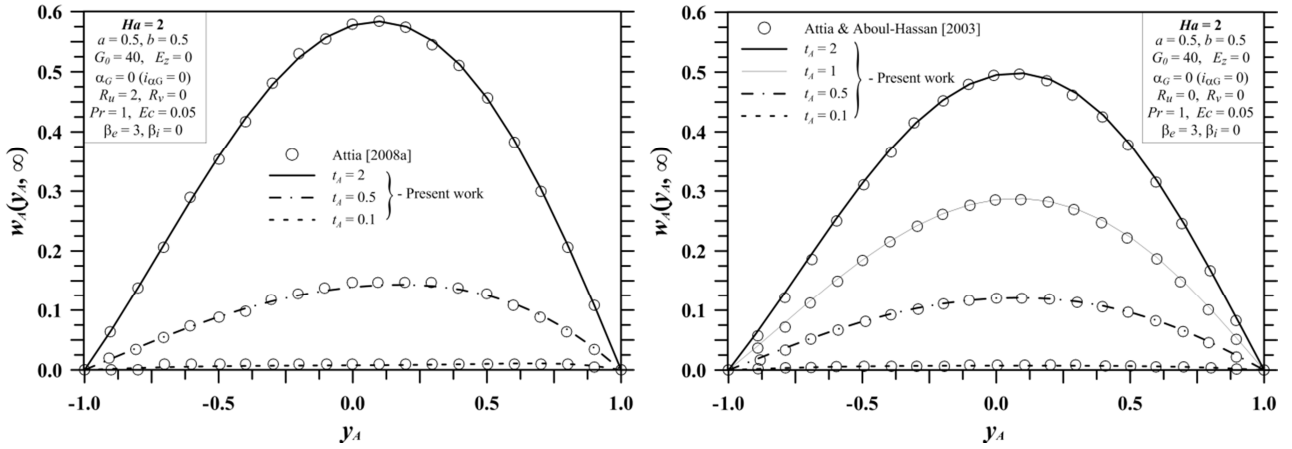


Figure 3. Transversal velocity profiles for the unsteady (a) Couette and (b) plane-Poiseuille flow at different times for $Ha = 2$.

To illustrate the direct influence of the applied magnetic field on the flow field, Figs. 4 and 5 show the velocity component profiles for generalized Couette and plane-Poiseuille configurations for $Ha = 6$.

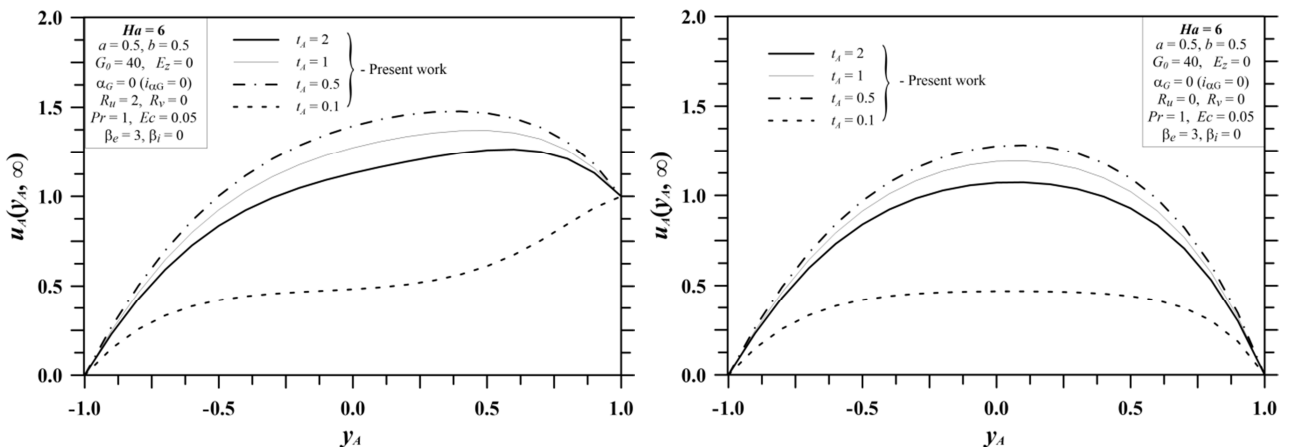


Figure 4. Longitudinal velocity profiles for the unsteady (a) Couette and (b) plane-Poiseuille flow at different times for $Ha = 6$.

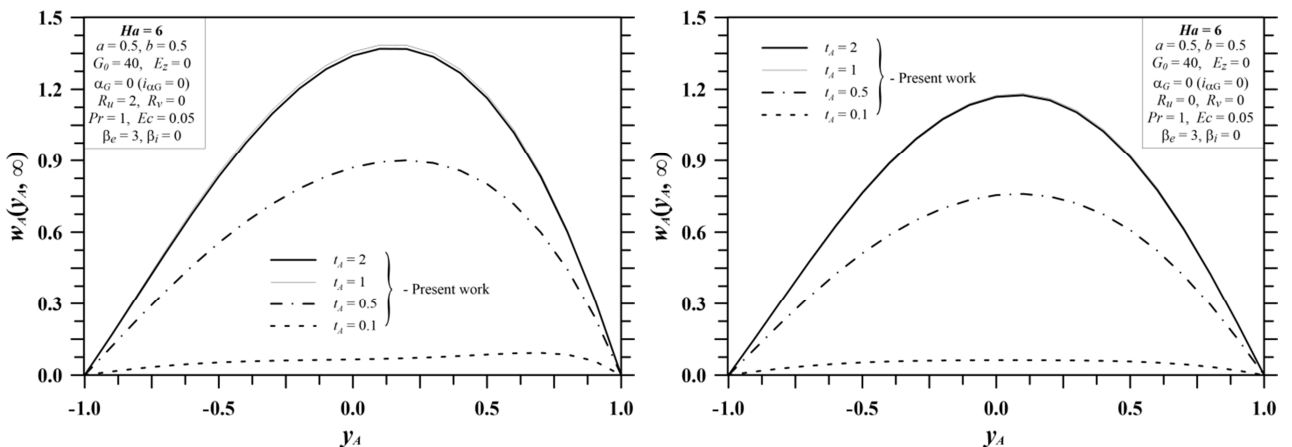


Figure 5. Transversal velocity profiles for the unsteady (a) Couette and (b) plane-Poiseuille flow at different times for $Ha = 6$.

These figures clearly show the strong influence of the magnetic field on the velocity components. For the situations analyzed, the retarding Lorentz force almost reduces the longitudinal velocity component to half of its original value and practically doubles the Hall effects on the transversal velocity component. Another interesting effect showed by these figures is that the velocity profiles present an overshooting behavior with the time evolution, *i.e.*, at some instant of time they exceed their steady-state values. Also, although not showed, the magnetic field presents a strong flattening effect on the temperature profile, as for the velocity field, especially when the steady-state regime is being reached.

Figures 7, 8 and 9 illustrate the dynamics of the longitudinal and transversal velocity components, and temperature, respectively, at the center of the channel for different values of the Hall parameter, β_e , showing the relation of this parameter to the overshooting phenomenon. Figures 7.a, 8.a and 9.a refer to $Ha = 6$ and Figures 7.b, 8.b and 9.b refers to $Ha = 10$. Comparisons are performed with the data of Attia & Aboul-Hassan [2003] for plane-Poiseuille flow.

These figures reveal that the overshooting phenomenon is strongly related to large values of Hartmann and Hall parameters and, more than this, the steady-state regime is not monotonically reached, *i.e.*, the velocity profiles present an oscillatory-type behavior for small instants of time and then go to the terminal state. Although magnitude of the velocity components is more attenuated, its occurrence is more evident for high Hartmann and Hall parameters.

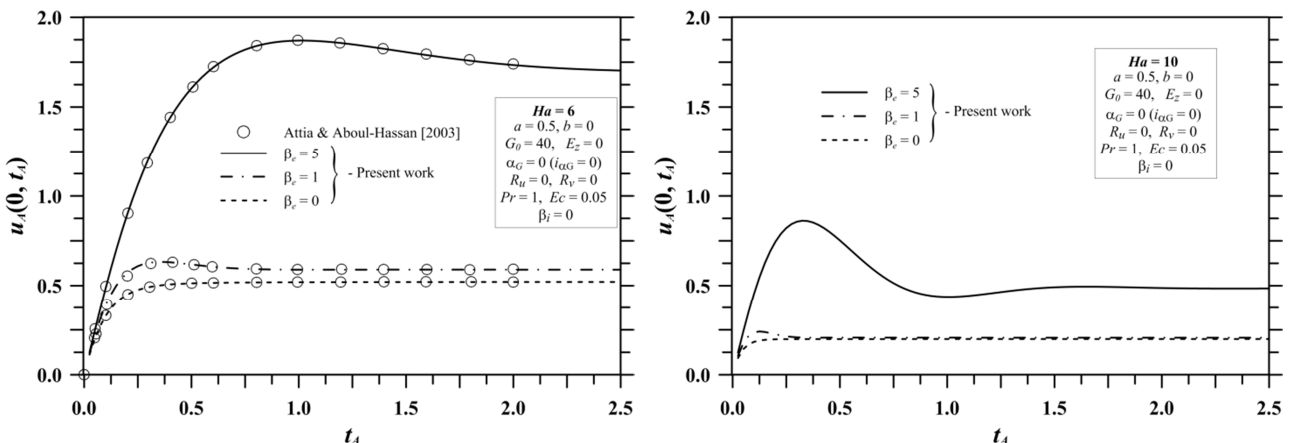


Fig. 7. Evolution of the centerline longitudinal velocity of the unsteady Hartmann flow for different values of Hall parameter and Hartmann number, β_e and Ha .

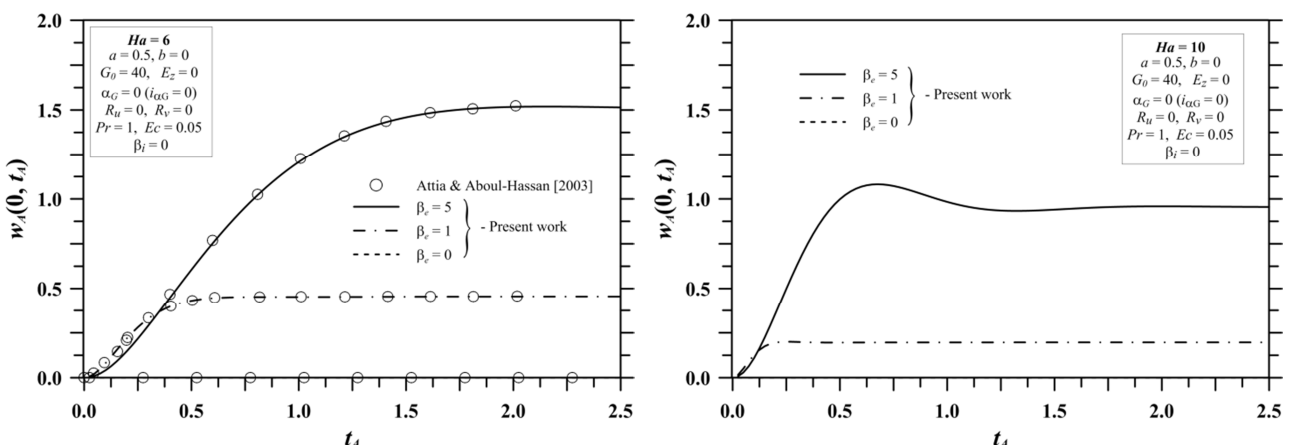


Fig. 8. Evolution of the centerline transversal velocity of the unsteady Hartmann flow for different values of Hall parameter and Hartmann number, β_e and Ha .

These figures also show that the time at which the longitudinal velocity component reaches its terminal steady-state regime increases with the Hall parameter, β_e . This is because this parameter governs the evolution of the transversal velocity component, which takes more time to develop, and as a consequence, the flow takes longer to arrive at the terminal state.

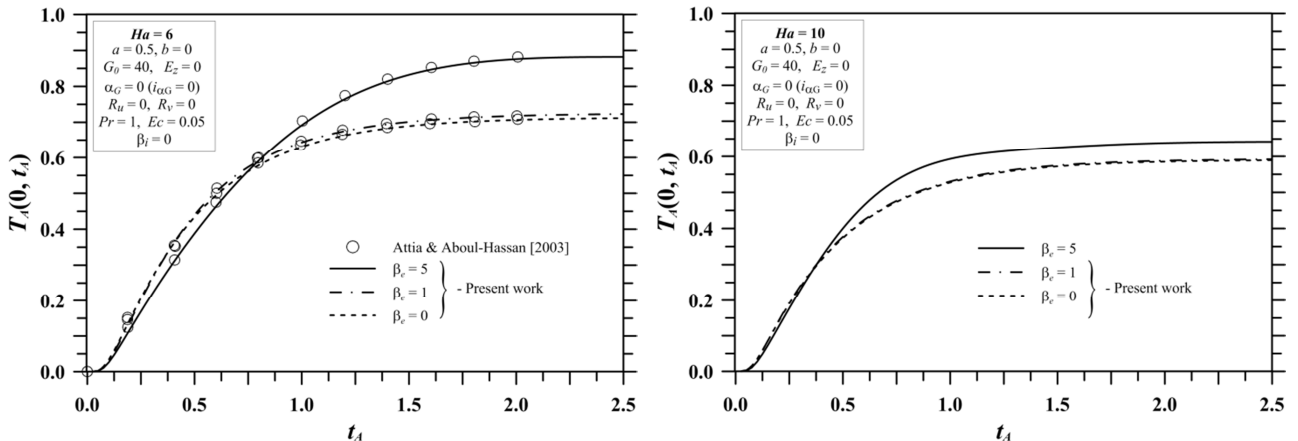


Fig. 9. Evolution of the centerline temperature of the unsteady Hartmann flow for different values of Hall parameter and Hartmann number, β_e and Ha .

In addition to the overshooting phenomenon, another interesting behavior is revealed by Figs. 7 and 8 for small times. Although the Hall parameter, β_e , is the drive parameter for the transversal velocity component, w , at small times and for large values of β_e , an increasing in β_e produces a decrease in w . Attia & Aboul-Hassan [2003] and Attia [2005a] explain this behavior showing that at small times, w is very small, so that part of the source term related to the Hall effect of the transversal velocity can be approximated to $\beta_e u/(1+\beta_e^2)$, which decreases (and so does w) when increasing β_e . A similar behavior is also visualized in Fig. 9 for the centerline temperature evolution and the same analysis is extended for the source term relative to the Joule dissipation in the energy equation.

Hall and ion-slip effects are now simultaneously accounted and the present hybrid results are compared to the data of Attia [2003], who analyzed the steady Hartmann flow with heat transfer and variable viscosity, and to the findings of Attia [2006b], who considered the unsteady Hartmann flow with heat transfer within two porous plates under an exponential decaying pressure gradient and constant properties. Where not explicitly stated, the following values were employed for the dimensionless parameters: $Ha = 6$, $G_o = 40$, $R_u = 0$, $Pr = 1$, $Ec = 0.05$, $E_z = 0$, $a = 0$, $b = 0$, $c = 0$.

Figures 10 to 12 show the effect of the Hall and the ion-slip parameters (β_e and β_i) on the steady-state longitudinal and transversal velocities and temperature profiles for $R_v = 0$ and $\alpha_G = 0$ ($i_{\alpha G} = 0$), and for two values of the Hartmann parameter ($Ha = 6$ and $Ha = 10$).

Except for the temperature profiles, the present results match the numerical ones of Attia [2003] for all parameters of Hall and ion-slip parameters analyzed. The differences between the results for the temperature field are attributed to a wrong mathematical description of the Joule dissipation term in the energy equation in the work of Attia [2003] (the expression $(1 + \beta_e \beta_i)$ must not be present in his mathematical formulation). This mistake is later corrected in the work of Attia [2006], although, there, he forgot to multiply his Joulean dissipation term by the Eckert parameter.

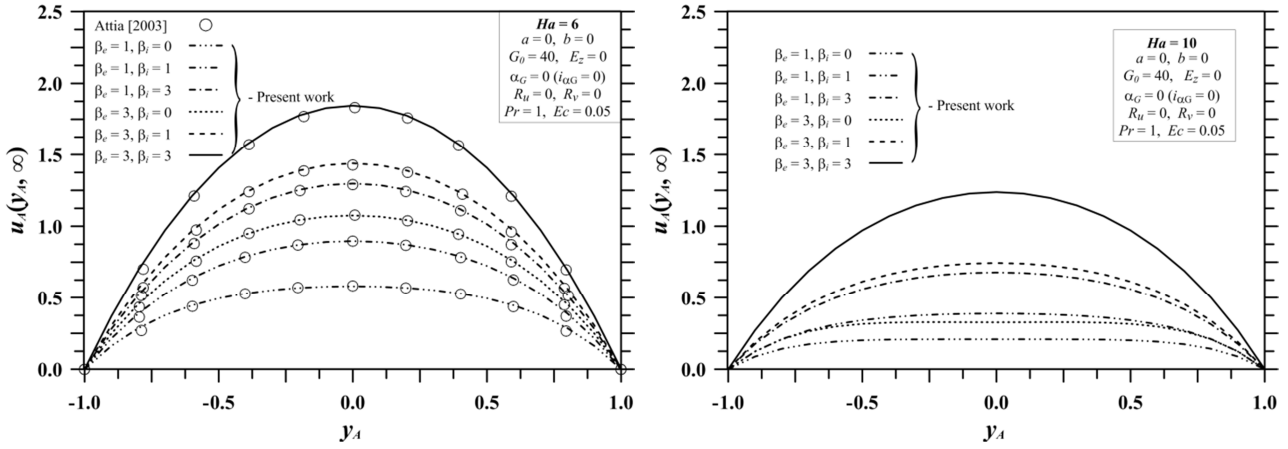


Figure 10. Axial velocity component profiles for the steady-state Hartmann flow for different values of Hartmann, Ha , and Hall and ion-slip parameters, β_e and β_i .

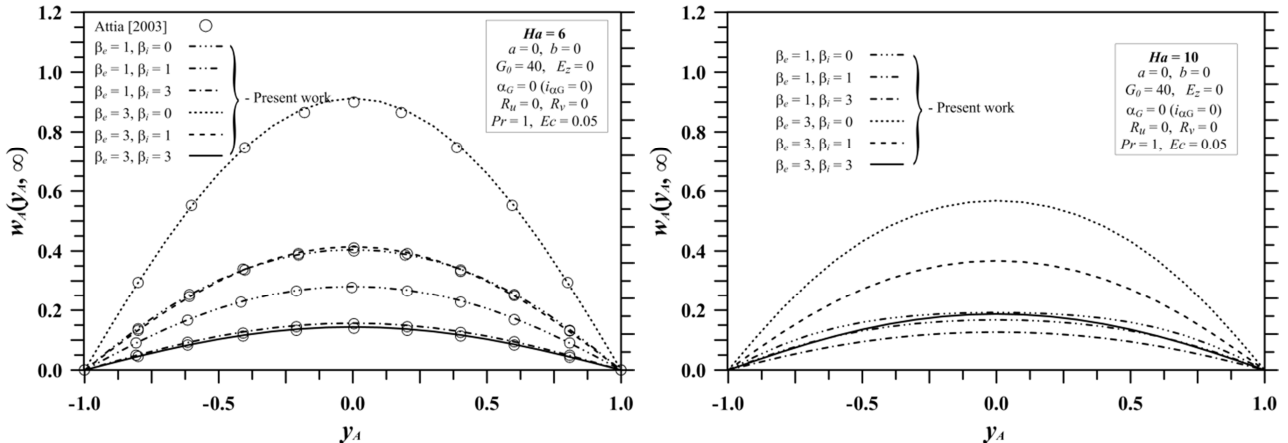


Figure 11. Axial velocity component profiles for the steady-state Hartmann flow for different values of Hartmann, Ha , and Hall and ion-slip parameters, β_e and β_i .

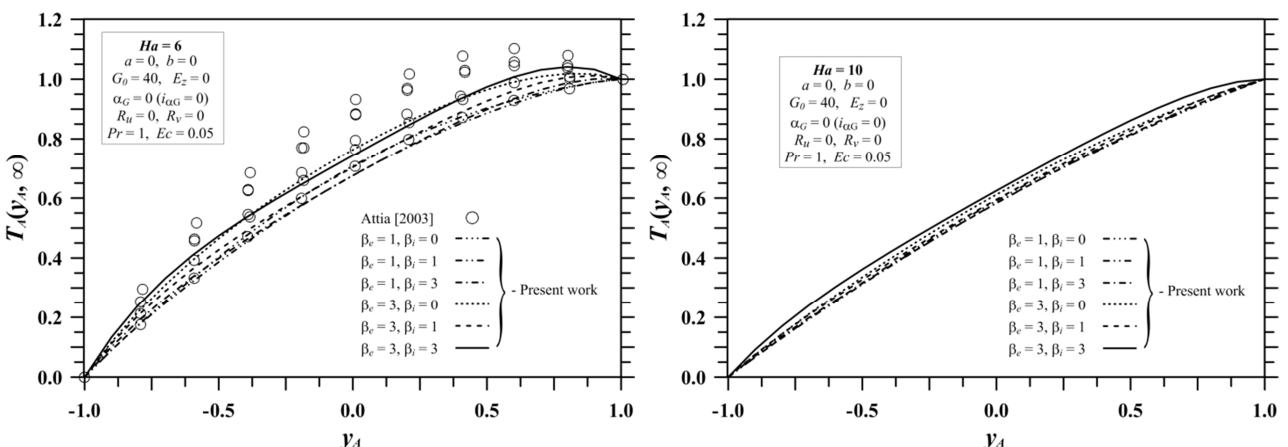


Figure 12. Temperature profiles for the steady-state Hartmann flow for different values of Hartmann, Ha , and Hall and ion-slip parameters, β_e and β_i .

Regarding to the influence of the Hartmann parameter on flow and temperature fields under the presence of both Hall and ion-slip effects, these figures ratify the same trends of the retarding effect of the Lorentz force observed in the previous figures on the flow and temperature fields. In relation to the Hall and ion-slip effects on the flow field, figures show that increasing the Hall (β_e) or the ion-slip (β_i) parameters increases u . An increase on β_e or β_i reduces the electrical conductivity, and so the Lorentz retarding force on u . In general, increasing β_e increases the transversal velocity, w , since it is the result of the Hall effect. On the other hand, increasing β_i produces a decreasing on w because this parameter decreases its source term and increases its damping term on the momentum equations [Attia, 2003].

Table 2 shows the results obtained with the present approach and illustrates some comparisons for the steady-state skin friction coefficients (longitudinal and transversal) and Nusselt number at both channel walls for different values of the ion-slip and viscosity parameters. Comparisons are performed with the results of Attia [2003].

Results clearly show the symmetry of the velocity field through the opposite values of the axial and transversal skin friction coefficients. An increasing in the ion-slip parameter (β_i) increases the axial skin friction coefficient (and the Nusselt number at the bottom plate) but decreases the transversal one. A changing of sign of the Nusselt number at the top wall is noticed when the ion-slip parameter is increased for low values of the Hall parameter. For higher values of the Hall parameter, increasing β_i has the effect of making the Nusselt number more negative, eliminating the change of sign.

Table 2

Steady-state skin friction coefficients and Nusselt number for different values of β_e and β_i and $Ha = 6$, $G_o = 40$, $R_u = 0$, $Pr = 1$, $Ec = 0.05$, $E_z = 0$, $a = 0$, $b = 0$, $c = 0$.

β_e	β_i	τ_{xA0}		τ_{xAl}		τ_{yA0}		τ_{yAl}	
		Present	Attia[2003]	Present	Attia[2003]	Present	Attia[2003]	Present	Attia[2003]
1	0	1.857	1.857	- 1.857	- 1.857	0.7308	0.732	- 0.7308	- 0.732
	0.5	2.142	2.385	- 2.142	- 2.385	0.5866	0.483	- 0.5866	- 0.483
3	0	2.728	-	- 2.728	-	1.509	-	- 1.509	-
	0.5	3.022	-	- 3.022	-	0.9857	-	- 0.9857	-
β_e	β_i	Nu_{A0}				Nu_{Al}			
		Present	Attia[2003]	Present	Attia[2003]	Present	Attia[2003]	Present	Attia[2003]
1	0	0.9294	0.935			0.07061	0.065		
	0.5	0.9303	1.139			0.06973	- 0.139		
3	0	1.253	-			- 0.2530	-		
	0.5	1.183	-			- 0.1825	-		

This table also reveals some small discrepancies between the hybrid results and those of Attia [2003]. We believe the results presented by Attia [2003] are not fully converged. It is important to know that the present results, for the steady-state regime, were obtained from evolution of the unsteady steady situation. Then, to show that the present results are converged and that use of the filtering procedure by the integral transform method brings an additional advantageous, Table 3 illustrates a convergence analysis for the skin friction coefficient and Nusselt number for the situation in which comparisons with the results of Attia [2003] were performed.

As one can see from Table 3, the integral transform results are fully converged for three significant algorithms. In addition, the ability of the filtering procedure in automatically recover the steady-state solution for the flow field (requiring few or no number of terms) demonstrates the analytical nature and flexibility of the GITT approach.

On the other hand, since the filter employed for the temperature field is not representative of the steady-state regime, it is necessary higher numbers of terms, especially for variable involving gradients, like the Nusselt number.

Table 3
Convergence analysis for the steady-state skin friction coefficients
and Nusselt number for two case analyzed in Table 2

β_e	β_i	N	τ_{xA0}	τ_{yA0}	Nu_{A0}	Nu_{A1}
1	0	10	1.857	0.7296	0.8995	0.1005
		50	1.857	0.7308	0.9240	0.07597
		100	1.857	0.7308	0.9272	0.07276
		200	1.857	0.7308	0.9289	0.07114
		300	1.857	0.7308	0.9294	0.07061
	Attia [2003]		1.857	0.732	0.935	0.065
	0.5	10	2.142	0.5858	0.8930	0.1070
		50	2.142	0.5866	0.9236	0.07638
		100	2.142	0.5866	0.9276	0.07239
		200	2.142	0.5866	0.9295	0.07040
		300	2.142	0.5866	0.9303	0.06973
	Attia [2003]		2.385	0.483	1.139	- 0.139

Results for the unsteady Hartmann flow with heat transfer within two porous plates under an exponential decaying pressure gradient and are now illustrated and compared. Again, when not explicitly stated, the following values were employed for the dimensionless parameters: $Ha = 6$, $G_o = 40$, $R_u = 0$, $\alpha_G = 4$ ($i_{\alpha G} = 1$), $Pr = 1$, $Ec = 0.05$, $E_z = 0$, $a = 0$, $b = 0$, $c = 0$.

Figure 13 illustrates the dynamics of the longitudinal and the transversal velocity components at the channel center for $R_v = 0$ and different combinations of the Hall and ion-slip parameters, β_e and β_i . Figure 14, on the other side, brings the same evolution of these variables but now showing the influence of the wall porosity, for $\beta_e = 3$ and different combinations of the wall suction/injection and ion-slip parameters (R_v and β_i).

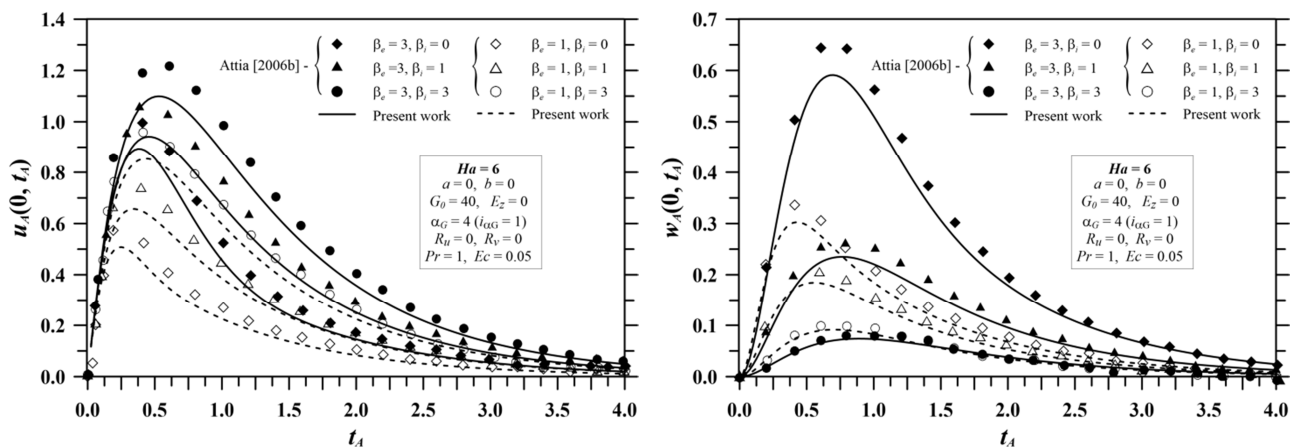


Figure 13. Evolution of the (a) centerline axial and (b) transversal velocities for different values of the ion-slip parameter, β_i , under an exponentially decaying pressure gradient.

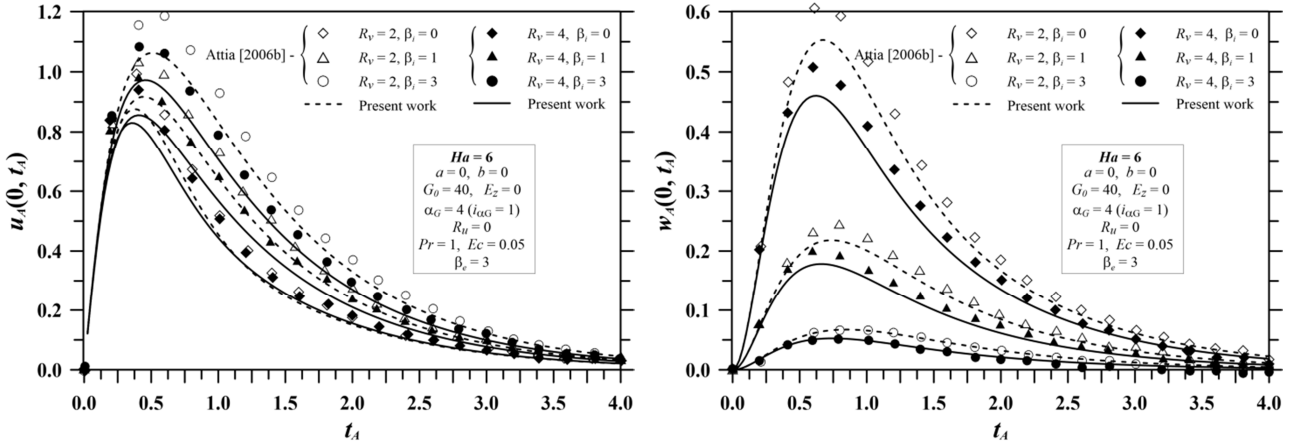


Figure 14. Evolution of the centerline axial and transversal velocities for different values of the ion-slip and wall porosity parameters (β_i, R_v), under an exponentially decaying pressure gradient.

In spite of some differences be present between the present results and those of Attia [2006b] the overall agreement is good. In order to show the accuracy of the main results obtained with the present approach, Table 4 depicts a convergence analysis for the axial and transversal velocity components results showed in Figs. 13 and 14, at selected instants of time.

Table 4

Convergence behavior of the velocity components at select instants of time for different values of β_i and $Ha = 6, G_o = 40, R_u = 0, R_v = 0, Pr = 1, Ec = 0.05, \beta_e = 3, E_z = 0, a = 0, b = 0, c = 0$.

N	$u_A(0, t_A)$							
	$t_A = 0.25$		$t_A = 0.5$		$t_A = 1.0$		$t_A = 2.0$	
	$\beta_i = 0$	$\beta_i = 3$						
10	0.8155	0.8812	0.8556	1.098	0.4574	0.8842	0.1455	0.3575
50	0.8146	0.8802	0.8549	1.098	0.4569	0.8837	0.1454	0.3573
100	0.8146	0.8802	0.8549	1.098	0.4569	0.8837	0.1454	0.3573
300	0.8146	0.8802	0.8549	1.098	0.4569	0.8837	0.1454	0.3573
$w_A(0, t_A)$								
10	0.2668	0.02566	0.5360	0.05716	0.5108	0.07302	0.1790	0.03782
50	0.2668	0.02566	0.5360	0.05716	0.5108	0.07302	0.1790	0.03782
100	0.2668	0.02566	0.5360	0.05716	0.5108	0.07302	0.1790	0.03782
300	0.2668	0.02566	0.5360	0.05716	0.5108	0.07302	0.1790	0.03782

Few terms are required to attain the convergence of the velocity components in the fourth digit. In reality, the transversal velocity component is already converged with only 10 terms in the expansion series for all instant of time illustrated. This table shows that only 50 terms is necessary for convergence of all potentials. Results provided by Attia [2006b] certainly may be contaminated with some kind of numerical errors.

Regarding to computational costs, for $N < 50$ only few seconds are necessary to run the code, while for intermediary number of terms, $N = 100$, its necessary about 3 minutes. Above 100 terms, for example, for the highest number of terms in the series, $N = 300$, it took about 30 minutes to be executed in an Intel I5, 1.7 GHz computer with 4 GB of memory. If the adaptive procedure [Santos *et al.*, 2001] had been employed, the time consumption would certainly be lower.

CONCLUSIONS

The outstanding potential of the integral transform method to handle problems where strong coupling and non-linearity are present is demonstrated in the present work. One can easily realize the strong flexibility introduced by the filtering process, when simplified versions of the problem being solved is used, at first, to homogenize boundary condition, but also bring the additional gain of reducing the requirement of terms in the eigen-expansions in regions/instants where the filtering expression is representative, for example, the steady-state or fully developed region in channel flows. In these situations, for certain values of the dimensionless parameters, there is no need of additional series summation, once the solution is the analytical filtering function itself.

Also, although not employed in the present work, previous works that made use of the integral transform have successfully implemented an adaptive procedure, where the terms in the series summations (and thus the size of the ODE system to be solved) is dynamically and progressively reduced along the time. This procedure can be easily implemented in the type of problem studied in this work.

Finally, the convergence analyses clearly showed how very small terms in the series solution are required to provide results with excellent accuracy. Low time consuming is a characteristic of the GITT approach for small terms in the eigen-expansions.

Therefore, these unique hybrid characteristics make the Generalized Integral Transform Technique an appropriate tool for benchmarking purposes in the field of magnetohydrodynamics, where strong current densities and body forces are responsible for modifications of the flow, temperature and magnetic fields. Integral transform solutions of problems where flow induces internal magnetic fields and these, in its turn, modify the applied one (for high magnetic Reynolds numbers) are currently object of research.

REFERENCES

- Attia, H.A. [1999], Transient MHD Flow and Heat Transfer between Two Parallel Plates with Temperature Dependent Viscosity, *Mec. Res. Comm.*, Vol. 26, No. 1, pp 115-121.
- Attia. H.A. [2002], Unsteady MHD Flow and Heat Transfer of Dusty Fluid between Parallel Plates with Variable Physical Properties, *App. Math. Modelling*, Vol. 26, pp 863-875.
- Attia, H.A. [2003], Steady Hartmann Flow with Temperature Dependent Viscosity and the Ion Slip, *Int. Comm. Heat Mass Transfer*, Vol. 30, No. 6, pp 881-890.
- Attia. H.A. [2005a], Magnetic Flow and Heat Transfer in a Rectangular Channel with Variable Viscosity, *The Arab. J. Sci. Eng.*, Vol. 30, No. 2A, pp 1-12.
- Attia. H.A. [2005b], Unsteady Flow of a Dusty Conducting Fluid between Parallel Porous Plates with Temperature Dependent Viscosity, *Turk. J. Phys.*, Vol. 29, pp 257-267.
- Attia. H.A. [2005c], Effect of the Ion Slip on the MHD Flow of a Dusty Fluid with Heat Transfer under Exponential Decaying Pressure Gradient, *Central Eur. J. Phys.*, Vol. 3, No. 4, pp 484-507.
- Attia, H.A. [2006a], Steady MHD Couette Flow with Temperature-Dependent Physical Properties, *Arch. Appl. Mech.*, Vol. 75, pp 268-274.

Attia, H.A. [2006b], Ion Slip Effect on Unsteady Hartmann Flow with Heat Transfer under Exponential Decaying Pressure Gradient, *Math. Prob. Eng.*, pp 1-12.

Attia, H.A. [2006c], Unsteady MHD Couette Flow and Heat Transfer of Dusty Fluid with Variable Physical Properties, *App. Math. Comp.*, Vol. 177, pp 308-318.

Attia, H.A. [2008a], The Effect of Variable Properties on the Unsteady Couette Flow with Heat Transfer considering the Hall effect, *Comm. Nonlinear Sci. Num. Sim.*, Vol. 13, pp 1596-1604.

Attia, H.A. [2008b], Unsteady hydromagnetic Couette Flow of Dusty Fluid with Temperature Dependent Viscosity and Thermal Conductivity under Exponential Decaying Pressure Gradient, *Comm. Nonlinear Sci. Num. Sim.*, Vol. 13, pp 1077-1088.

Attia, H.A. & Aboul-Hassan, A.L. [2003], The Effect of Variable Properties on Unsteady Hartmann Flow with Heat Transfer Considering the Hall Effect, *Appl. Math. Modelling*, Vol. 27, pp 551-563.

Attia, H.A. & Kotb, N.A. [1996], MHD Flow between Two Parallel Plates with Heat Transfer, *Acta Mechanica*, pp 215-220.

Attia, H.A., Abbas, W. & Abdeen, M.A.M. [2015], Ion Slip Effect on Unsteady Couette Flow of a Dusty Fluid in the Presence of Uniform Suction and Injection with Heat Transfer, *J. Braz. Soc. Mech. Sci. Eng.*, DOI 10.1007/s40430-015-0311-y.

Cotta, R.M. [1993], *Integral Transforms in Computational Heat and Fluid Flow*, CRC Press, Boca Raton, FL, USA.

Cotta, R.M. [1998], *The Integral Transform Method in Thermal and Fluid Science and Engineering*, Begell House Inc, NY, USA.

Cotta, R.M. & Mikhailov, M.D. [1997], *Heat Conduction: Lumped Analysis, Integral Transforms, Symbolic Computation*, John Wiley & Sons, Chichester, WS, England.

Davidson, P.A. [2001], *An Introduction to Magnetohydrodynamics*, Cambridge University Press, New York, USA.

Hwang, C.L., Li, K.C. & Fan, L.T. [1966], Magnetohydrodynamic Channel Entrance Flow with Parabolic Velocity at the Entry, *The Physics of Fluids*, Vol. 9, No. 6, pp 1134-1140.

IMSL Library [2010], *Math/Lib*, Visual Numerics Inc., Houston, Texas, USA.

Lima, J.A., Quaresma, J.N.N. & Macêdo, E.N. [2007], Integral Transform Analysis of MHD Flow and Heat Transfer in Parallel-Plate Channels, *Int. Comm. Heat Mass Transfer*, Vol. 34, No. 4, pp 420-431.

Lima, J.A. & Rêgo, M.G.O. [2013], On the Integral Transform Solution of Low-Magnetic MHD Flow and Heat Transfer in the Entrance Region of a Channel, *Int. J. Non-Linear Mech.*, Vol. 50, pp 25-39.

Mikhailov, M.D. & Ozisik, M.N. [1984], *Unified Analysis and Solutions of Heat and Mass Diffusion*, Dover Edition, Toronto, Canada.

Ozisik, M.N. & Murray, R.L. [1974], On the Solution of Linear Diffusion Problems with Variable Boundary Condition Parameters, *ASME J. Heat Transfer*, Vol. 96, Series C, No. 1, pp 48-51.

Santos, C.A.C, Quaresma, J.N.N. & Lima, J.A. [2001], *Convective Heat Transfer in Ducts: The Integral Transform Approach*, E-Papers, Rio de Janeiro, RJ, Brazil.

Setayesh, A. & Sahai, V. [1990], Heat Transfer in Developing Magnetohydrodynamic Poiseuille Flow and Variable Transport Properties, *Int. J. Heat Mass Transfer*, Vol. 33, No. 8, pp 1711-1720.

Shercliff, J.A. [1965], *A Textbook of Magnetohydrodynamics*, Pergamon Press, London, UK.

Shohet, J.L., Osterle, J.F. & Young, F.J. [1962], Velocity and Temperature Profiles for Laminar Magnetohydrodynamic Flow in the Entrance Region of a Plane Channel, *The Physics of Fluids*, Vol. 5, No. 5, pp 545-549.

Sutton, G.W. and Sherman, A. [2006], *Engineering Magnetohydrodynamics*, Dover Publications Inc., Mineola, New York, USA.

Wolfram, S. [2010], *Mathematica: A System for Doing Mathematics by Computer*, Addison-Wesley, USA.